Rev.Adv.Mater.Sci. 25 (2010) 16-22

LIMITATIONS IN THE REFINEMENT BY SEVERE PLASTIC DEFORMATION: THE EFFECT OF PROCESSING

A. Bachmaier[1], M. Hafok[1], R. Schuster[2] and R. Pippan[1,3]

[1]Erich Schmid Institute of Materials Science – Austrian Academy of Sciences, Jahnstr.12, A-8700 Leoben, Austria
[2]Institute of Materials Physics, University of Vienna, A-1090 Wien, Austria
[3]Christian Doppler Laboratory for Local Analysis of Deformation and Fracture, Jahnstr.12, A-8700 Leoben, Austria

Received: November 27, 2009

Abstract. High Pressure Torsion (HPT) is a simple and effective severe plastic deformation method to produce ultrafine grained or even nanocrystalline microstructures. However, at a certain applied strain no further refinement of the microstructure occurs. HPT deformation of bulk Ni at room temperature leads to a typical saturation microstructure with a mean grain size of approximately 200 nm. In the present work, it will be shown that additional heavy cold rolling of a saturation microstructure does not help to overcome this limit. Furthermore, a strategy to bypass this limitation in the grain refinement using HPT deformation is presented. The main key lies in the reduction of grain boundary migration during the deformation. Thus bulk nanocrystalline Ni samples with an average grain size below 30 nm can be produced.

1. INTRODUCTION

Severe plastic deformation is a well known procedure for producing significant grain refinement in bulk materials. High pressure torsion (HPT) is one of these severe plastic deformation techniques which allows the application of a large amount of strain in a simple way.

In literature, a lot of reports concerning the HPT deformation of bulk Ni and the structural evolution during the deformation can be found [1-4]. If a high enough amount of strain is applied, a saturation in the refinement process occurs and a microstructure with a mean grain size of approximately 200 nm can be obtained by HPT deformation of Ni at room temperature. Once this so-called saturation region is reached, it is impossible to further decrease the grain size by processing the samples to higher strains if the HPT deformation is conducted at room temperature [3,5,6]. Nevertheless, the deformation temperature as well as the purity of the processed material influence the size of the grains in the saturation region [4].

If HPT is applied to Ni single crystals, a similar saturation microstructure is reached [7,8]. The limitation in the refinement becomes even more clearly visible if HPT deformation is applied to Ni which has an initial nanocrystalline structure with a mean grain size of approximately 20 nm [9]. The HPT deforma-

Corresponding author: A. Bachmaier, e-mail: andrea.bachmaier@stud.unileoben.ac.at

tion induces grain growth and the nanocrystalline structure is transformed into an ultrafine grained structure with a final grain size of approximately 200 nm.

Independent of the initial state of the material before the HPT deformation, always the same saturation grain size is reached in the aforementioned examples. It apparently seems to be impossible to overcome the limit in the structural refinement during HPT deformation of pure bulk Ni.

Nevertheless, Ni with an average grain size less than 10 nm has been produced by a repeated rolling and folding process [10,11]. Although the applied amount of strain is similar during HPT, the minimum grain size in Ni obtained by the repeated rolling and folding process is more than one order of magnitude finer than that in HPT processed Ni.

The present work is devoted to the question if a different strain path like in the repeated rolling and folding process leads to a different saturation grain size. Moreover a way to further reduce the minimum grain size achievable by HPT deformation is presented.

2. EXPERIMENTAL

A detailed description of the HPT equipment used for processing the materials present in this paper is given in [12]. The shear strain γ_{HPT} during HPT deformation can be calculated according to

$$\gamma_{HTP} = \frac{2\pi n}{t} r , \qquad (1)$$

whereby r, n, t are the distance from the center of the sample, the number of rotations and the thickness of the sample, respectively. The von Mises equivalent shear strain ε_{vHPT} is then given by [13]

$$\varepsilon_{vHTP} = \frac{\gamma_{HTP}}{\sqrt{3}}. \qquad (2)$$

Disk shaped Ni (99.5 %) samples with a diameter of 30 mm and a height of 10 mm were HPT deformed at room temperature for 10 rotations. This corresponds to a ε_{vHPT} of 32 at a radius of 14 mm. The pressure during the deformation was 2.8 GPa and the rotation speed was kept constant at 0.2 rpm. The thus processed material is denoted as initial HPT state. A part of these HPT deformed bulk Ni samples was further treated by the following methods.

State 1 was obtained by cold rolling of the HPT deformed bulk Ni sample in a single standard cold rolling mill with 83% thickness reduction after the HPT deformation. State 2 was achieved by the same cold rolling process of the HPT deformed bulk Ni sample with 96% thickness reduction. To evaluate the additional amount of strain, the von Mises equivalent strain for rolling deformation, ε_{CR}, was calculated by

$$\varepsilon_{CR} = \frac{2}{\sqrt{3}} \ln\left(\frac{t_0}{t_f}\right), \qquad (3)$$

whereby t_0 and t_f are the thickness of the sample before and after the cold rolling, respectively. The calculation of the additional amount of equivalent strain for rolling deformation gives a ε_{CR} of 2.1 and 3.7 for State 1 and 2, respectively. The total strain ε for State 1 and 2 is calculated by the addition of ε_{vHPT} and ε_{CR}. State 1 was deformed to a ε of 34.1 and State 2 to a ε of 35.7 if the von Mises equivalent shear strain ε_{vHPT} of the initial HPT deformed sample is calculated at a radius of 14 mm. If one considers a volume element at a radius of 7 mm ε_{vHPT} is 16 and the total strain ε is 18.7 and 19.7 for State 1 and 2, respectively.

Furthermore, Nickel powder (99.9%, 3-7 microns from Alfa Aesar®) which was additionally annealed before the compaction was processed by HPT. The precompacted samples with a diameter of 14 mm and a thickness t of 0.8 mm were deformed by HPT at room temperature. The pressure during deformation was 5 GPa and the rotation speed was kept constant at 0.2 rpm.

Microstructures were characterized in a scanning electron microscope (SEM) type LEO 1525 using back scattered electrons and in a transmission electron microscope (TEM) type Philips CM12. The microtexture was investigated by electron back scatter diffraction (EBSD) using the EBSD system attached to the SEM. The direction of observation is given in Fig. 1a. All microstructural investigations in the cold rolled sheets were carried out on the normal direction (ND)- rolling direction (RD) planes. Vickers microhardness measurements were performed on a BUEHLER Mircomet 5100 using a load of 1000 g.

The HPT Ni powder consolidated samples have been subjected to multi reflection X-ray line profile analysis using synchrotron radiation available at the Synchrotron ELETTRA, Trieste, Italy. From the crystallite size distribution, which can be described by a log-normal function, the area weighted mean crystallite size $\langle x \rangle_{area}$ was obtained [14].

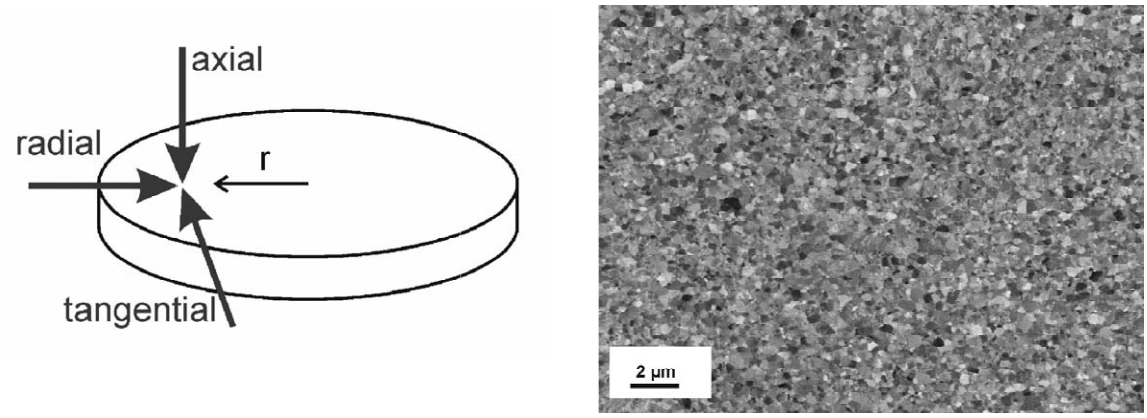

Fig. 1. (a) Definition of the direction of observation, (b) the microstructure of the bulk Ni sample HPT deformed at room temperature to an equivalent shear strain ε_{vHPT} of 32 observed in tangential direction.

3. RESULTS AND DISCUSSION

In the case of HPT deformation of pure Ni, a saturation in the refinement is observed between an equivalent shear strain ε_{vHPT}=8 and 16 [5]. The deformation condition and the applied strain were chosen for the microstructure to be in the saturation region for all samples. The Ni discs were deformed by HPT at room temperature to a corresponding equivalent shear strain ε_{vHPT} of 32 at a radius of 14 mm. The resulting saturation microstructure after the HPT deformation in tangential direction at a radius of 14 mm is shown in Fig. 1b. The micrograph shows a typical saturation microstructure. In tangential and axial direction, the grains have an equiaxed shape within the saturation region. In radial direction, an elongation of the grains with a preferred direction of the grains somewhat inclined in the shear direction can be observed [5]. Grain sizes were measured by linear intersection method in horizontal and vertical direction. The mean grain size using this approach in horizontal and vertical direction is 225 nm and 227 nm, respectively. It is important to notice that the grain size cannot be decreased further by applying higher strains once the saturation region is reached.

To examine if the application of a different strain path can lead to a finer saturation grain size, the inital HPT deformed Ni samples were cold rolled to two different additive shear strains. Fig. 2a shows the microstructure of the sample which was additionally cold rolled to an equivalent shear strain ε_{CR} of 2.1 (State 1), resulting in a total equivalent shear strain ε of 34.1. Compared to the initial microstructure shown in Fig. 1b, the grains become aligned in the rolling direction and an elongation of the grains in the rolling direction is also clearly visible. Therefore, the thickness of the elongated grains becomes

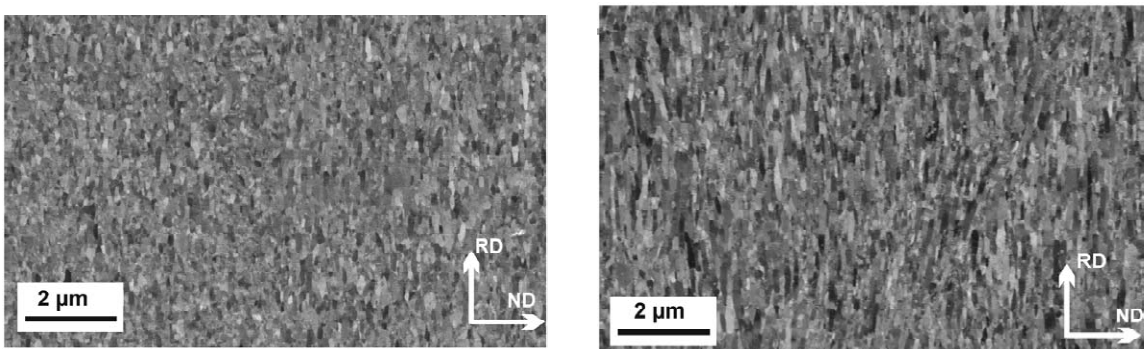

Fig. 2. (a) The microstructures of the bulk Ni sample which were additionally cold rolled after HPT deformation with 83% reduction and (b) with 96% reduction. The rolling direction (RD) and normal direction (ND) during the cold rolling is depicted in the lower right corner.

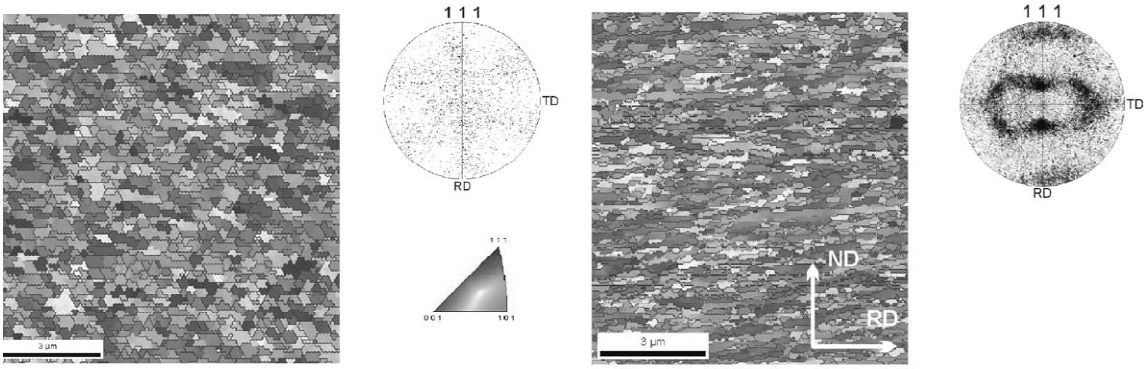

Fig. 3. (a) Electron back scattered diffraction (EBSD) map in the radial direction at a radius of about 6 mm (ε_{vHPT} = 32) and the corresponding pole figure in the [111] direction. The standard triangle used for the EBSD maps is given in the lower right corner, (b) EBSD map of HPT deformed Ni which was additionally cold rolled with 83% reduction and the corresponding pole figure in the [111] direction. The rolling direction (RD) and normal direction (ND) during the cold rolling is depicted in the lower right corner of the micrographs.

somewhat smaller compared to the inital state after HPT deformation due to the deformation. Nevertheless, the elongation is much less than expected from a simple elongation due to the rolling. The mean grain size measured by lineal intersection method is 205 nm in normal direction and 406 nm in rolling direction. Fig. 2b shows the microstructure of the cold rolled sample which experienced an additional equivalent shear strain ε_{CR} of 3.7 (State 2). Although the amount of the additional applied equivalent shear strain ε_{CR} in State 2 is nearly two times more than in State 1, no significant difference in the microstructure between the two states is visible and the observed thickness reduction does not correlate with the applied reduction of the rolled sheets. It rather seems that after a certain amount of cold rolling the grain size reaches a saturation again and no further refinement of the microstructure takes place.

Fig. 3a shows the inverse pole figure map of HPT deformed Ni at an equivalent shear strain ε_{vHPT} of 32 which was obtained in radial direction. Each color corresponds according to the standard triangle to a specific crystallographic orientation. The pole figure in the [111] direction of the sample shows a torsion shear texture which is typical for HPT deformation [8].

The inverse pole figure of the Ni sample which was additionally cold rolled with 83% thickness reduction after the HPT deformation and the corresponding pole figure in the [111] direction are shown in Fig. 3b. Considerable differences between the texture of the HPT deformed Ni sample and the sample which was additionally cold rolled can be observed. After cold rolling, the texture is similar to one typically obtained by cold rolling of pure Ni [15,16].

Considering the aforementioned results the different strain path in the repeated rolling and folding process and HPT deformation can not solely be responsible for the significant finer saturation grain size in the rolling and folding process. In literature, different explanations for the occurrence of the saturation in the grain refinement during processing have been proposed. Besides grain boundary sliding or localized deformation, grain boundary migration is proposed to be the dominant process responsible for the limitation in the refinement by severe plastic deformation [17]. If boundary migration limits the refinement during severe plastic deformation, introducing second phase or nano particles during processing should make it possible to stabilize finer microstructure.

Therefore, HPT consolidation and deformation of oxidized Ni powders were performed to introduce oxides in the latter bulk compacts. These oxides should act as barriers for boundary migration during the deformation process. To get a sufficiently thick oxide layer on the particle surface before the HPT consolidation, an annealing treatment was performed before the compaction. The annealing treatment was carried out in air at 400 °C for 10 minutes. Afterwards the powder was precompacted directly in the HPT tool and subsequently deformed at room temperature. Fig. 4a shows a bright field

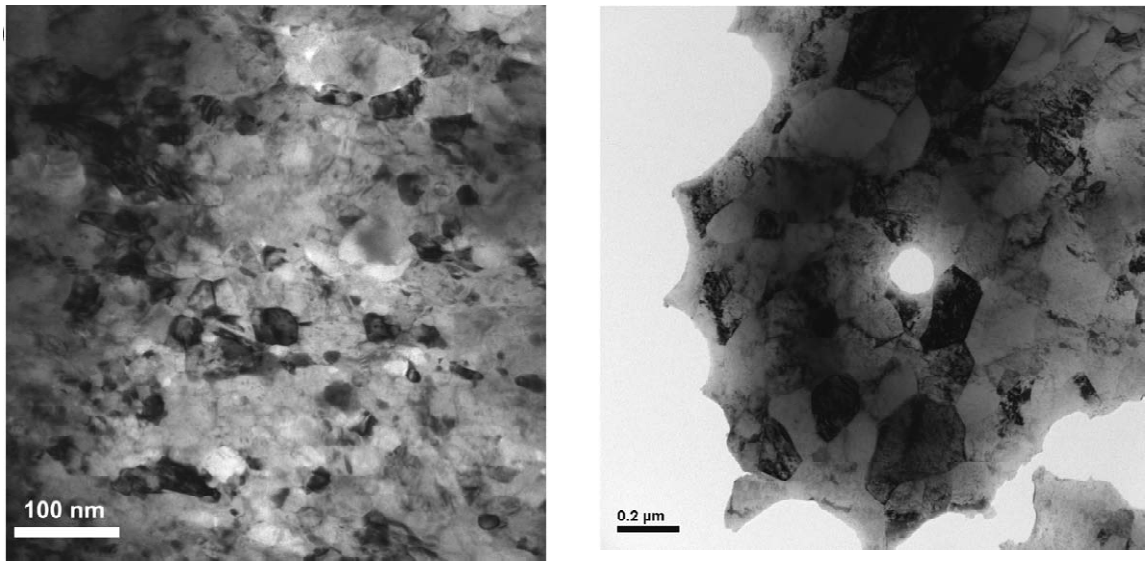

Fig. 4. (a) Bright-field transmission electron micrograph of the microstructure of the HPT consolidated sample of oxidized Ni powder [18], (b) bright-field transmission electron micrograph of the microstructure of the HPT deformed sample of bulk Ni. Please note the difference in magnification.

TEM image of the resulting saturation microstructure of the HPT consolidated sample of oxidized Ni powder [18]. Compared to the bright field TEM image of the saturation microstructure of the HPT bulk Ni sample shown in Fig. 4b, a significant smaller grain size can be seen. Indeed, a nanocrystalline structure is revealed. XRD measurements confirmed a two phase structure consisting of Ni and a small quantity of NiO in the HPT consolidated sample of oxidized Ni powder. Fig. 5a shows the XRD pattern of the HPT consolidated sample of oxidized Nickel powder. In Fig. 5b the size distributions of the coherently scattering domains of the Ni and NiO phase are shown. From the size distribution, the area weighted mean crystallite size $\langle x \rangle_{area}$ can be determined. The values for $\langle x \rangle_{area}$ are 31 nm and 9 nm for the Ni and NiO phase, respectively. The grain size distribution measured using several TEM images gives a mean grain size of 29.8 nm with a standard deviation of 20.6 nm, whereas NiO particles cannot be distinguished from Ni matrix grains [18].

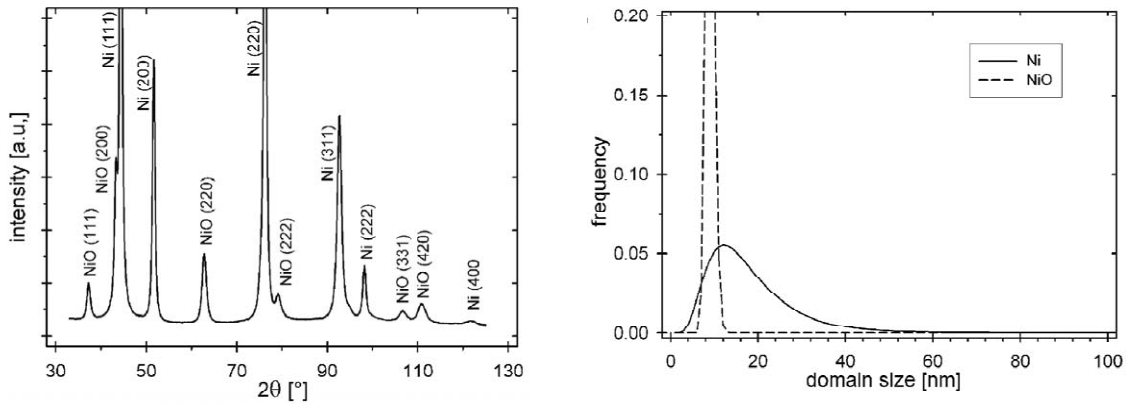

Fig. 5. (a) XRD pattern of HPT consolidated sample of oxidized Ni powder, (b) size distribution of the coherently scattering domains as determined by multiple X-ray Bragg profile analysis.

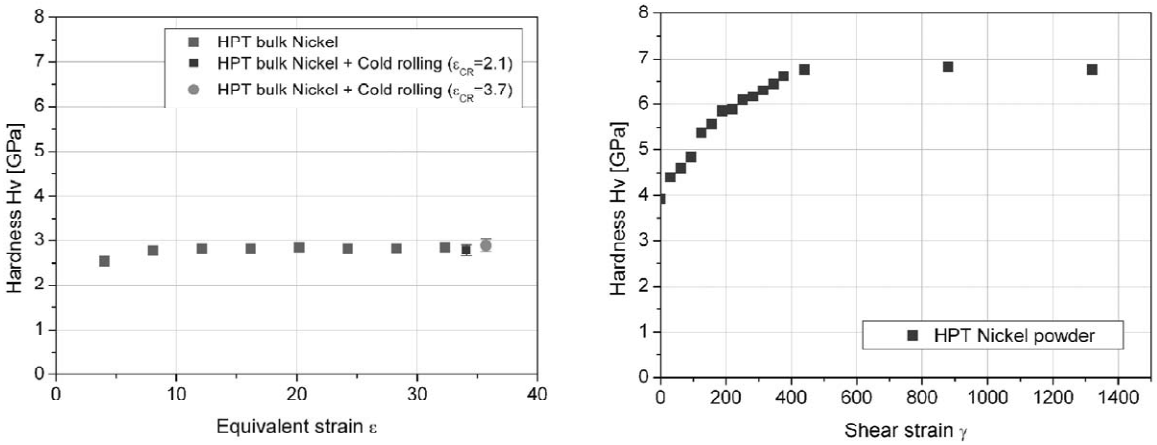

Fig. 6. (a) Microhardness of bulk HPT deformed Ni at room temperature as a function of the applied equivalent shear strain. The microhardness values of the Ni samples which were additionally cold rolled to two different strains are also shown. (b) Microhardness of HPT consolidated oxidized Ni powder sample as a function of the applied equivalent shear strain.

The differences, or comparing the initial HPT state and the cold rolled states, the similarities in the saturation microstructures are also reflected in the hardness values. Fig. 6a shows the evolution of the measured hardness values as a function of the applied equivalent shear strain in the HPT deformed bulk Ni and for the cold rolled samples. HPT deformation of bulk Ni leads to a hardness increase from 0.6 GPa in the undeformed state up to a hardness of 2.8 GPa in the saturation region. Additional cold rolling does not cause a significant further increase in the hardness. For the sample which was additionally cold rolled to an equivalent shear strain ε_{CR} of 2.1 (State 1), a hardness of 2.8 GPa was obtained. A hardness of 2.9 GPa was measured for the sample which was additionally cold rolled to an ε_{CR} of 3.7. Fig. 6b shows the evolution of the hardness as a function of the applied equivalent shear strain for the HPT consolidated samples of oxidized Ni powder. The HPT consolidated sample of oxidized Ni powder exhibits the highest hardness values (6.8 GPa) in the saturation region which is nearly 2.5 times the hardness of the HPT bulk Ni samples.

These results emphasize the importance of the introduced oxides on the refinement of the microstructure. Besides the effect on the refinement and the hardness, the thermal stability of the microstructure could also be clearly improved as shown in [18]. The same mechanism which impedes grain boundary migration during the deformation is also responsible for the improved thermal stability.

4. CONCLUSION

It could be shown that the large difference in the minimum size of the saturation microstructure after the different severe plastic deformation processes results not solely from the different applied strain paths. The dominant process which limits the grain refinement is the occurrence of grain boundary migration during severe plastic deformation. Therefore, to stabilize finer microstructures the movement of the grain boundaries must be hindered. In this work, it was possible to synthesize nanocrystalline bulk Ni using HPT deformation due to the pinning effect caused by the introduction of small oxide particles. These Ni oxide particles do not only lower the minimum achievable grain size, they also strengthen the matrix effectively and an excellent thermal structural stability is reached.

The financial support by the Austrian Fonds zur Förderung der wissenschaftlichen Forschung (Project number: S10402-N16) is gratefully acknowledged.

REFERENCES

[1] A.P. Zhilyaev, S. Lee, G.V. Nurislamova, R.Z. Valiev and T.G. Langdon // *Scripta Mater.* **44** (2001) 2753.

[2] A.P. Zhilyaev, G.V. Nurislamova, B.K. Kim, M.D. Baró, J.A. Szpunar and T.G. Langdon // *Acta Mater.* **51** (2003) 753.

[3] X. Huang, G. Winther, N. Hansen, T. Hebesberger, A. Vorhauer, R. Pippan and M. Zehetbauer // *Mater. Sci. Forum* **426-432** (2003) 2819.
[4] H. Zhang, X. Huang, R. Pippan and N. Hansen // *in press Acta Mater.*
[5] R. Pippan, F. Wetscher, M. Hafok, A. Vorhauer and I. Sabirov // *Adv. Eng. Mater.* **11** (2006) 1046.
[6] T. Hebesberger, H.P. Stüwe, A. Vorhauer, F. Wetscher and R. Pippan // *Acta Mater*. **410-411 (**2005) 281.
[7] M. Hafok and R. Pippan // *Philos. Mag*. **88** (2008) 1857.
[8] M. Hafok and R. Pippan // *Mater. Sci. Forum* **550** (2007) 277.
[9] B. Yang, H. Vehoff, H. Hohenwarter, M. Hafok and R. Pippan // *Scripta Mater.* **58** (2008) 790.
[10] G.P. Dinda, H. Rösner and G. Wilde // *Mater. Sci. Eng. A* **410-411** (2005) 328.
[11] G.P. Dinda, H. Rösner and G. Wilde // *Scripta Mater.* **52** (2005) 577.
[12] A. Vorhauer, S. Kleber and R. Pippan // *Mater. Sci. Eng.* A **410–411** (2005) 281.
[13] H.P. Stüwe // *Adv. Eng. Mater.* **5** (2003) 291.
[14] E. Schafler and R. Pippan // *Mater. Sci. Eng. A* **387-389** (2004) 799.
[15] R.R. Ray // *Acta Metall. Mater.* **43** (1995) 3863.
[16] J. Pospiech, J. Jura, A. Mücklich, K. Pawlik and M. Betzl // *Text. Microstruct.* **6** (1983) 63.
[17] R. Pippan, S. Scheriau, A. Taylor, M. Hafok, A. Hohenwarter and A. Bachmaier // *accepted for publication in Annu. Rev. Mat. Res.* (2010).
[18] A. Bachmaier, A. Hohenwarter and R. Pippan // *Scripta Mater.* **61** (2009) 1016.